

	
Project (Grant) Number:	824135
Project Acronym:	SOLARNET
Project Title:	Integrating High Resolution Solar Physics

Document Details	
Document Title:	Image Slicer Design
Prepared by (Institution’s Name):	Instituto de Astrofisica de Canarias (IAC)
Work Package number & Title:	WP6 - JRA2 Advanced Instrumentation Development
Deliverable Number & Title:	D6.1 - Image Slicer Design
Serial Number of Deliverable:	D55
Document code: (inserted by project office)	D6.1_Version 1.0
File name: (inserted by project office)	SOLARNET_D6.1_V1.0_ISD_Public_20200226
Date uploaded: (inserted by project office)	Feb 26 th , 2020

AUTHORS/ CONTRIBUTORS LIST

Name	Function	Organization
Carlos Dominguez	Research Scientist (sub-WP leader)	IAC
Álvaro Pérez García	Optical Engineer (Task Contributor)	IAC

SCIENTIFIC APPROVAL CONTROL FROM SUB-WP & WP LEAD

Control	Name	Organization	Function	Date
Prepared	Carlos Dominguez	IAC	Sub-WP leader	Feb 3 rd , 2020
Revised	Roberto Lopez	IAC	Senior Optical Engineer	Feb 21 st , 2020
Approved	Manolo Collados	IAC	WP6 leader	Feb 21 st , 2020

ADMINISTRATIVE APPROVAL CONTROL FROM PROJECT OFFICE

Control	Name	Organization	Function	Date
Approved	Tirtha Som	Leibniz-Institute for Solar Physics (KIS)	Project Manager	Feb 25 th , 2020
Approved	Rolf Schlichenmaier	KIS	Project Coordinator	Feb 25 th , 2020
Authorized	Markus Roth	KIS	Project Scientist	Feb 26 th , 2020

HISTORY OF DOCUMENT CHANGES

Issue	Date	Change Description
Version 1.0	Feb 26 th , 2020	Initial Issue

Table of Contents

1. Introduction.....	4
2. Optical design.....	4
2.1 Glass image slicer.....	5
2.2 Metallic image slicer.....	8
2.3 Expected performance.....	13
3. Conclusions.....	15

List of Abbreviations

EST	European Solar Telescope
GREST	Getting Ready for the EST project
FOV	Field of View
GRIS	GREGOR Infrared Spectrograph
IFU	Integral Field Unit
IAC	Instituto de Astrofísica de Canarias
NAOJ	National Astronomical Observatory of Japan
NINS	National Institutes of Natural Sciences
WO	Winlight Optics, in the next future will be Winlight System

1. Introduction

sWP6.1 has the objective of increasing the spatial resolution of the Integral Field Units (IFU) based on image slicers. The goal is to produce IFUs with slices thinner than the ones designed in the framework of previous project (RD1 and 2). That slicer was made of glass (Zerodur®) and had slices of 100 microns width, the thinnest elements ever built at that time. Now, in order to go thinner, two strategies are underworking: glass image slicers (produced by WO) and metallic image slicers (produced by the collaboration of NINS/NAOJ and Canon Inc.).

Two designs of the Image slicer have been developed in parallel, one for metallic slicers and a second one for glass slicers taking into account that the thickness of the first one could go down to 35 μm and the second one to 70 μm . The optical design heritages the concept of image slicers considered for the previous projects described in RD1 to 4. As well, the design is made compatible with the spectrograph GRIS at GREGOR solar Telescope (RD5) in order to test the prototype.

An additional objective included in this design is to demonstrate the multi-slit capabilities of image slicers, as heritage of the work in RD4. For this goal, one of the optical designs includes one image slicer divided in two sections, obtaining two slits but a continuous FOV. Each section of the image slicer, reflects the FOV towards two separate collimator and camera arrays, and therefore, two different overlapping pupil image planes are formed.

The optical design has been done in close collaboration with the partners WO, and NINS/NAOJ.

2. Optical design

The image slicer reorganizes the FOV in several mini-slits, going through an array of collimator mirrors and focusing with an array of camera mirrors. At the output, an array of several mini-slits is fed into a spectrograph. The design is optimized for the spectrograph GRIS (RD5), taking the common requirements described in Table 1.

The requirement of telecentricity implies that every mirror shares the same focal distance, and the pupil images for each slice have to be overlapped in a common plane. Therefore, the collimator and camera mirrors must be placed, maintaining a separation between slicer and collimator equal to focal distance, and two times the focal distance between collimator and camera mirrors. The coordinates where the pupils overlap is calculated averaging the theoretical pupil position for each collimator-camera system. The pupil mask is located at this place.

Table 1. Common requirements

Magnification	1
Illumination type	Telecentric
Main wavelengths	1083 nm & 1565 nm
Number of output slits	1-2
Detector size	1020 x 1024 pixels
Pixel size	18 μm

As described before, the thickness of the slicers will be 35 μm and 70 μm for the metallic and glass devices, respectively. For these thicknesses, diffraction effects have to be taken into account and the optical components must be sized accordingly, as the main diffractive lobe beam is greater than the geometrical one, in the diffractive direction. Table 2 summarizes the specifications of the optical design for both materials: metal and glass. The following two sections describe them in detail.

Table 2. Specifications

	Metal	Glass
Output slits	2	1
Slices	16	8
Useful FOV	2.1” x 4.4”	2.1” x 6,7”
Slice dimensions	0.035 mm x 1.176 mm	0.070 mm x 1.800 mm
Collimator and camera mirror dimensions	5.7 m x 13.4 mm	4.2 m x 3.3 mm
Collimator and camera mirror curvature	Spherical	Spherical
Mirror radius	300 mm	140 mm
Pupil masks	2	1
Folding mirrors	16	2
Folding mirror dimensions	3 mm x 3 mm	12 mm x 1.3 mm

2.1 Glass image slicer

The technology of image slicer made of glass (Zerodur®), already demonstrated by WO for a thickness of 100 µm, is pushed to go down to 70 µm (see RD6). The new optical design inherits the concept from RD1 and the goal to be compatible with the spectrograph GRIS. The new design improves the telecentricity and the focus differences among the mini-slits. Figure 1 shows the layout, which follows a Z-pattern, where the output is higher than the input to keep the same configuration in the instrument. In consequence, the camera mirrors are higher than the collimator ones. The differences in the position of the rows of these mirrors are to guarantee the telecentricity, as explained before. They are arranged in two rows in order to reduce the relative angle of the beams from the 8 slices. Reducing the angles minimizes the aberrations. The mirrors are grouped in two arrays of 4 elements (see Figure 2).

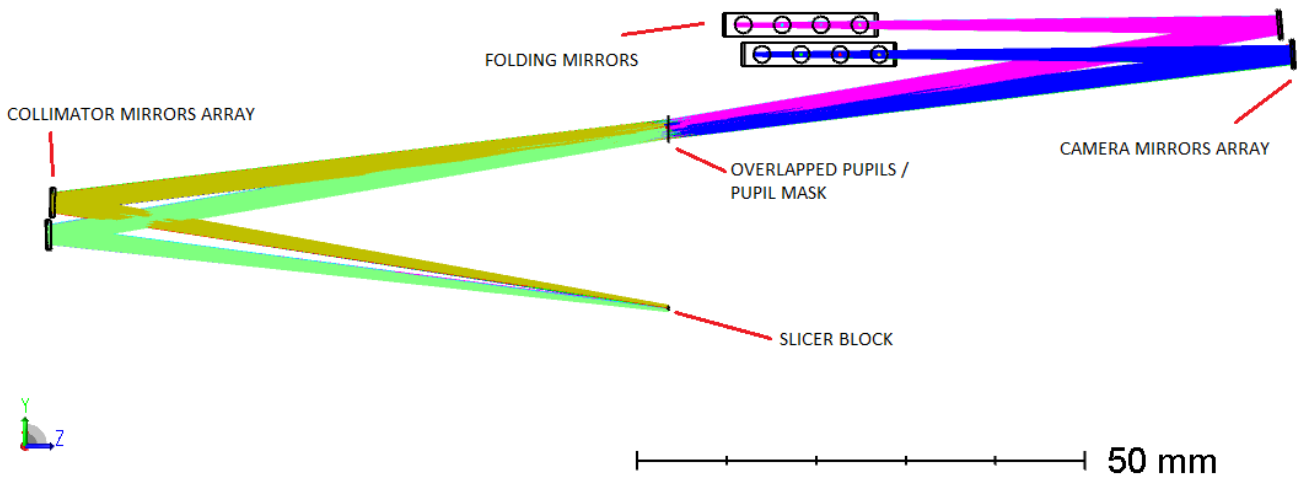


Figure 1 Layout of the glass slicer IFU, side view

The input light comes from the left side and focuses at the image slicer, which has 8 useful flat mirrors, plus 4 extra ones at the edges (not shown in the picture), to send their reflection out of the optical path. The slices distribute the light to top and bottom collimator mirrors, keeping to a minimum the relative angles between contiguous slices. This is done to reduce their shadow to the neighbour slice. Table 3 shows the slicer parameters from the Zemax file. The rotations are performed around the centre of each slicer mirror,

and they are defined as extrinsic rotations in the global coordinate system, due to the need to guarantee the absence of tilts over Z-axis.

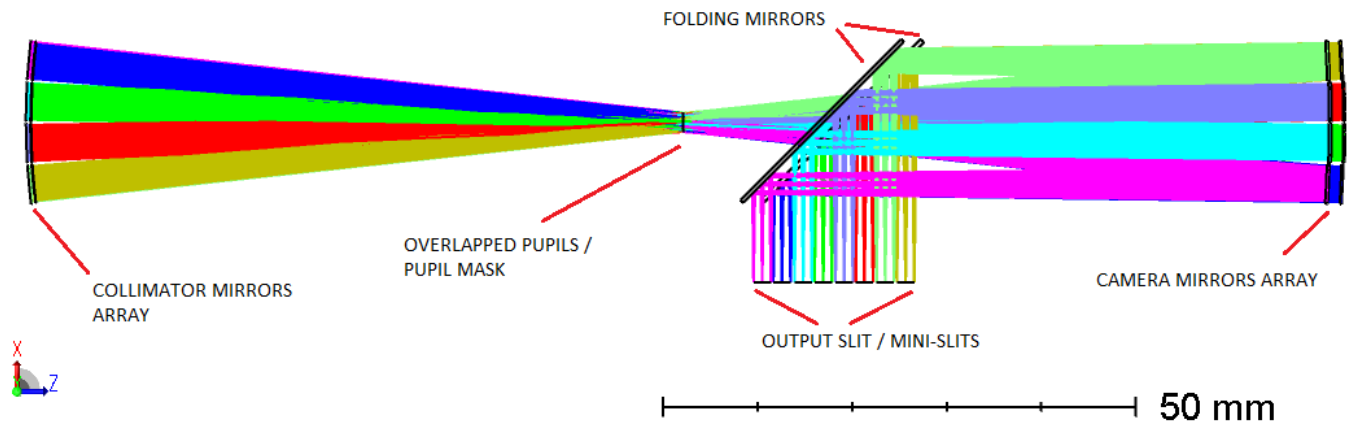


Figure 2 Top view

Table 3. Slicer array parameters

dec.X	dec.X	dec.X	dec.X	dec.X	dec.X	dec.X	dec.X
0,0000	0,0000	0,0000	0,0000	0,0000	0,0000	0,0000	0,0000
dec.Y	dec.Y	dec.Y	dec.Y	dec.Y	dec.Y	dec.Y	dec.Y
0,0350	0,1050	0,1750	0,2450	-0,0350	-0,1050	-0,1750	-0,2450
tilt X	tilt X	tilt X	tilt X	tilt X	tilt X	tilt X	tilt X
4,8390	4,8052	4,7761	4,7516	3,3860	3,4115	3,4404	3,4728
tilt Y	tilt Y	tilt Y	tilt Y	tilt Y	tilt Y	tilt Y	tilt Y
-2,6624	-0,8863	0,8862	2,6618	-2,7208	-0,9099	0,8976	2,7089

Due to the small thickness of the slices, diffraction effects have to be taken into account. Then, the collimator and following mirrors have to be sized accordingly. The minimum dimensions of the collimator mirrors are 4.2 mm width x 3.3 mm high. Figure 3 shows a comparison between the Zemax footprint and the diffractive beam simulation at one of the collimator mirrors.

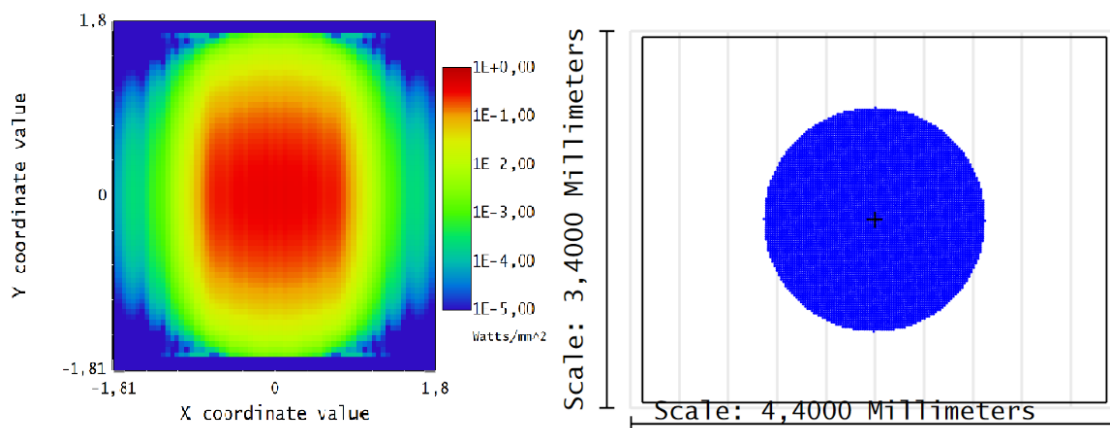


Figure 3 Diffraction simulation vs footprint at collimator

The diffraction effects are considered for the pupil mask as well. The IFU is designed for two different wavelengths, so that there are two different optimal diameters of pupil masks. A diameter of 3.12 mm corresponds to the main lobe diffractive beam diameter at the wavelength of 1565 nm, and 2.16 mm at 1083 nm.

The array of camera mirrors has the same concept than the collimator one. It is divided in two rows, as explained before. The separation between them is 3.3 mm, which is the same separation between the mini-slit rows of the output slit. This separation is constrained by the camera mirrors size. The folding mirror at the output is divided in two rows, in order to reduce the focal plane differences between the top and bottom mini-slits. This can be seen in Figure 4. Table 4 lists the focus difference to the image plane, for each mini-slit.

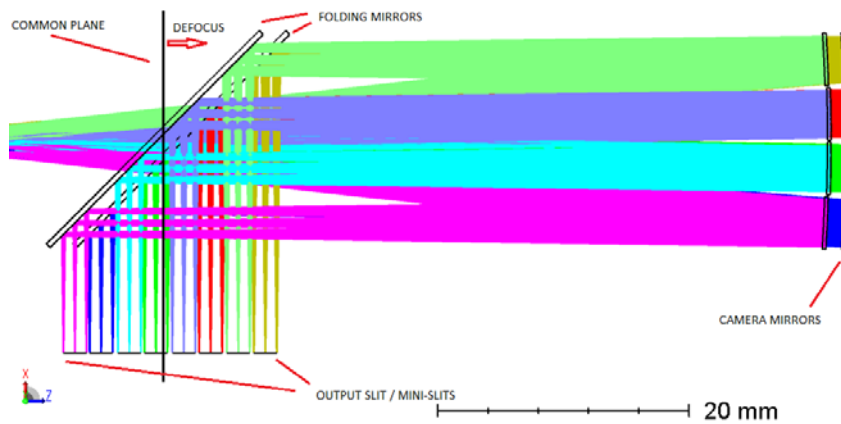


Figure 4 Folding mirrors and output slit

Table 4. Focus differences for the mini-slits

		INDIVIDUAL	FOCUS					
0,4357	0,1779	0,1905	0,4731	-0,1705	-0,4516	-0,4599	-0,1954	

The alignment of the mini-slits is very important and keeping the tilts to a minimum has placed constraints to the design. The mini-slits shall be perpendicular to the ruling of the spectrograph grating. A tilted slit, would produce a tilted spectra. The maximum tilt, respect to the horizontal axis, is lower than 0.009 mm. Figure 5 shows the footprint of all the mini-slits overlapped using 9 fields over the FOV. It also shows the way that the tilt is measured.

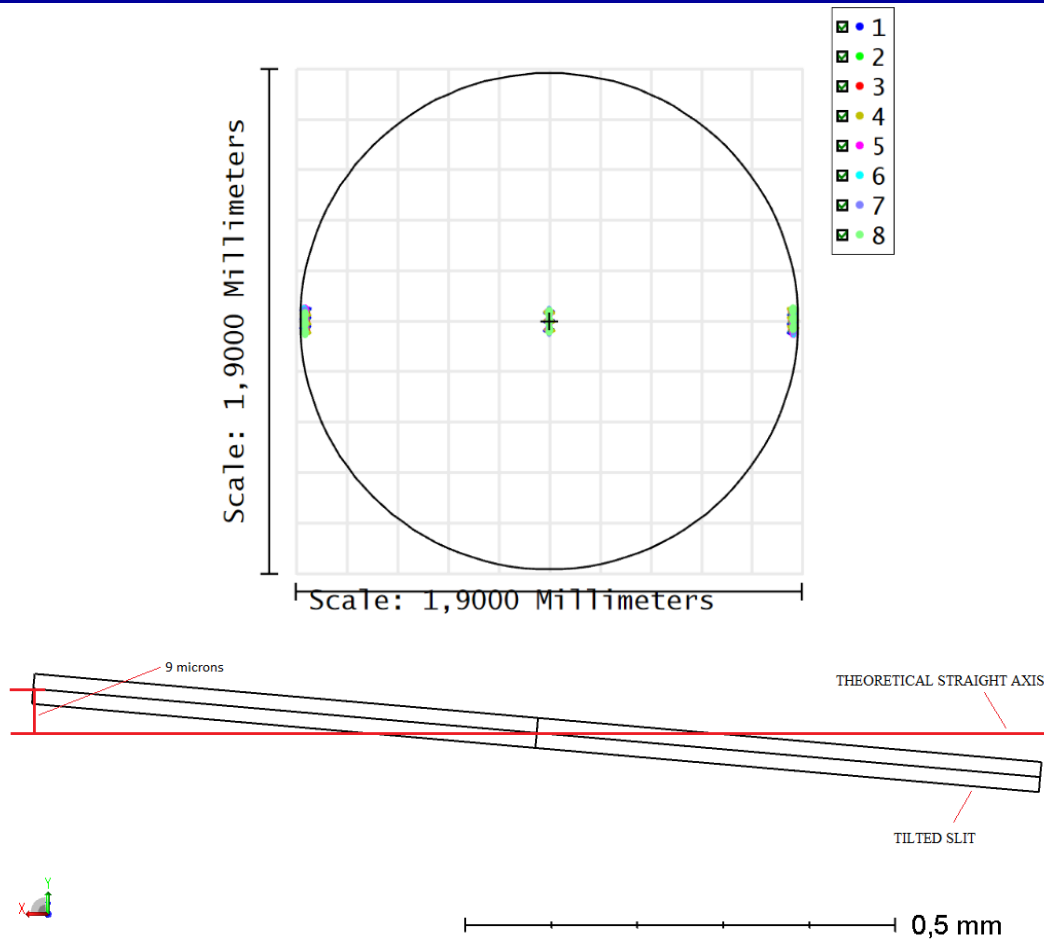


Figure 5 Maximum tilt of the mini-slits

2.2 Metallic image slicer

The technology developed by the collaboration of NINS/NAOJ and Canon Inc., allows to fabricate the slices in the material Zero Invar® (RD7) with thicknesses of 35 μm . With this thickness, the spatial resolution is increased but the FOV is greatly reduced, therefore the number of slices is augmented. This is a good candidate to test the image slicer divided in two sections to obtain two output slits. A larger number of slits implies bigger angles and more aberrations, then the focal distance of 150 mm for the camera and collimator mirrors was chosen, in order to minimize the angles in the slicer, to avoid vignetting factors and to reduce the aberrations. The consequence is the increase of divergence in the beams from the slicer to the collimator. This increment requires bigger mirrors for the collimator and camera, and a bigger separation between the mini-slits.

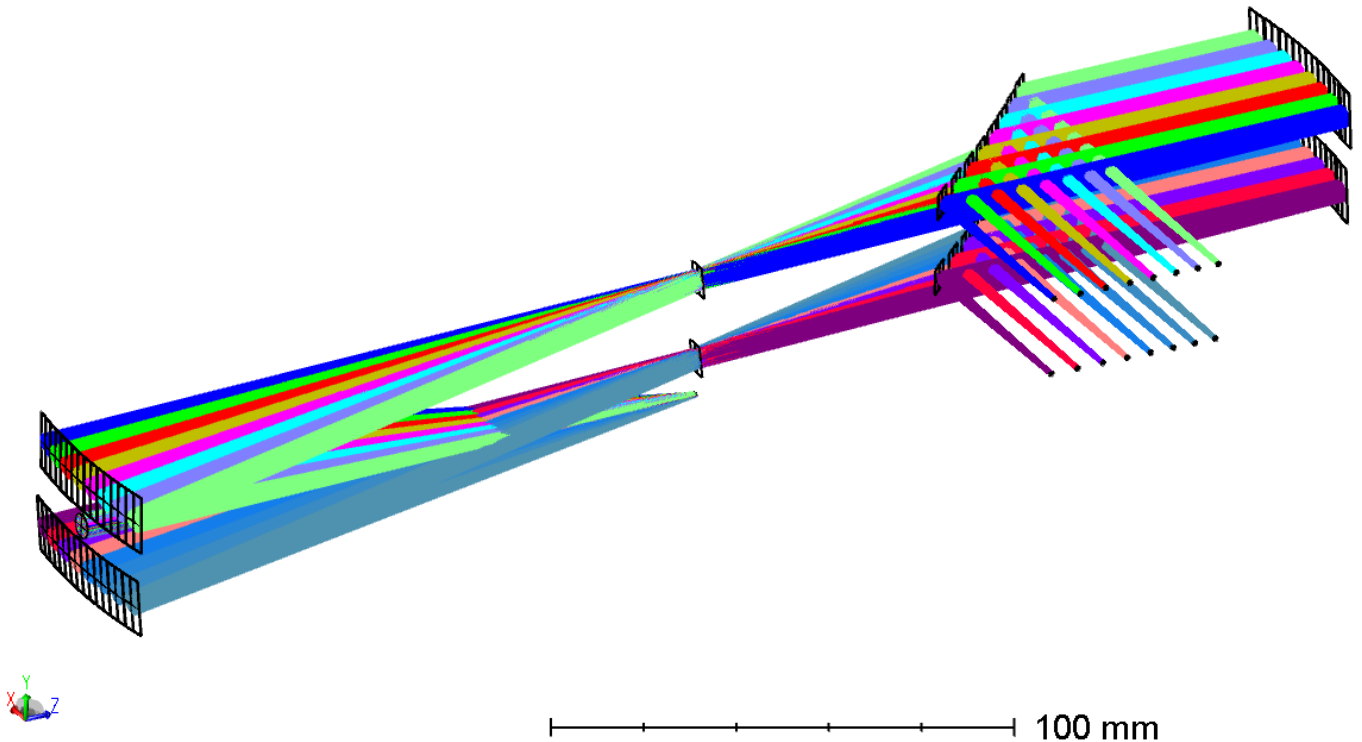


Figure 6 Layout of the metallic slicer IFU

As it can be seen in Figures 6 and 7, the layout follows two Z-patterns, where the camera mirrors are higher than the collimator ones. There are two main optical paths to form two slits. Two pupils are formed and two masks are required. RS2 mirror introduces the light into the system and is not part of the IFU optical design. However, RS2 is in the same plane as the collimator mirrors, then, it has to be integrated in the same block.

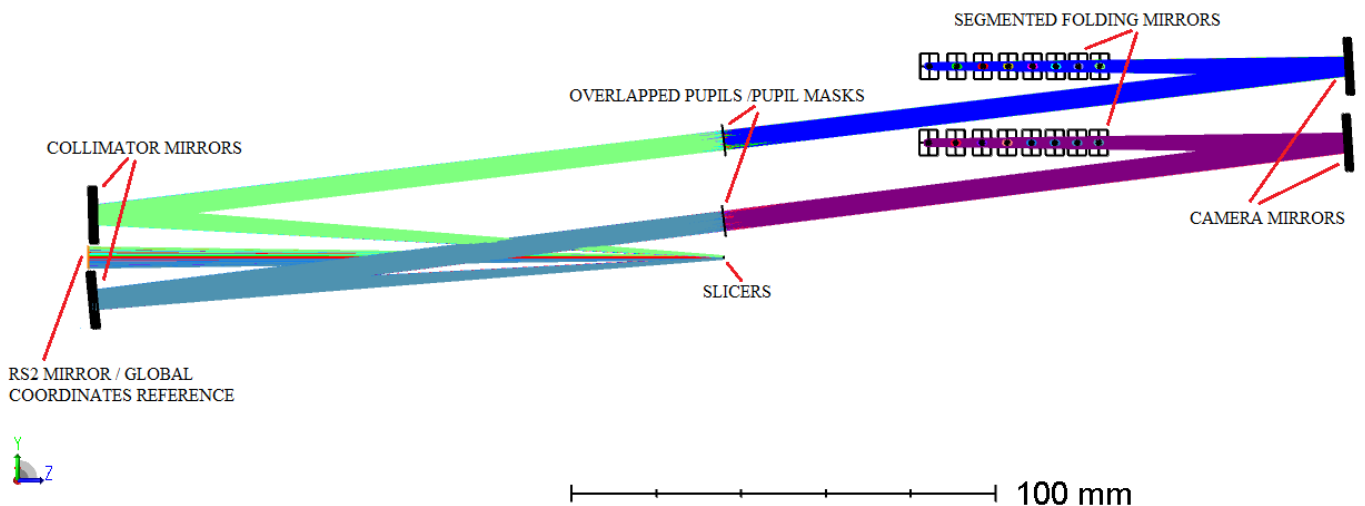


Figure 7 Side view

Figures 7 and 8, show how the folding mirror is divided in several segments, one for each camera mirror, in order to compensate the focal plane differences among the 16 mini-slits.

The image slicer has 16 useful flat mirrors, plus 4 extra ones (not shown in the pictures), at the edges. The slices distribute the light to the top and bottom rows of collimator mirrors, one row for each slit. Table 5 shows the slicer parameters from the Zemax file. The rotations are performed around the centre of each slicer mirror, and they are defined as extrinsic rotations in the global coordinate system, as in the case of the glass slicer.

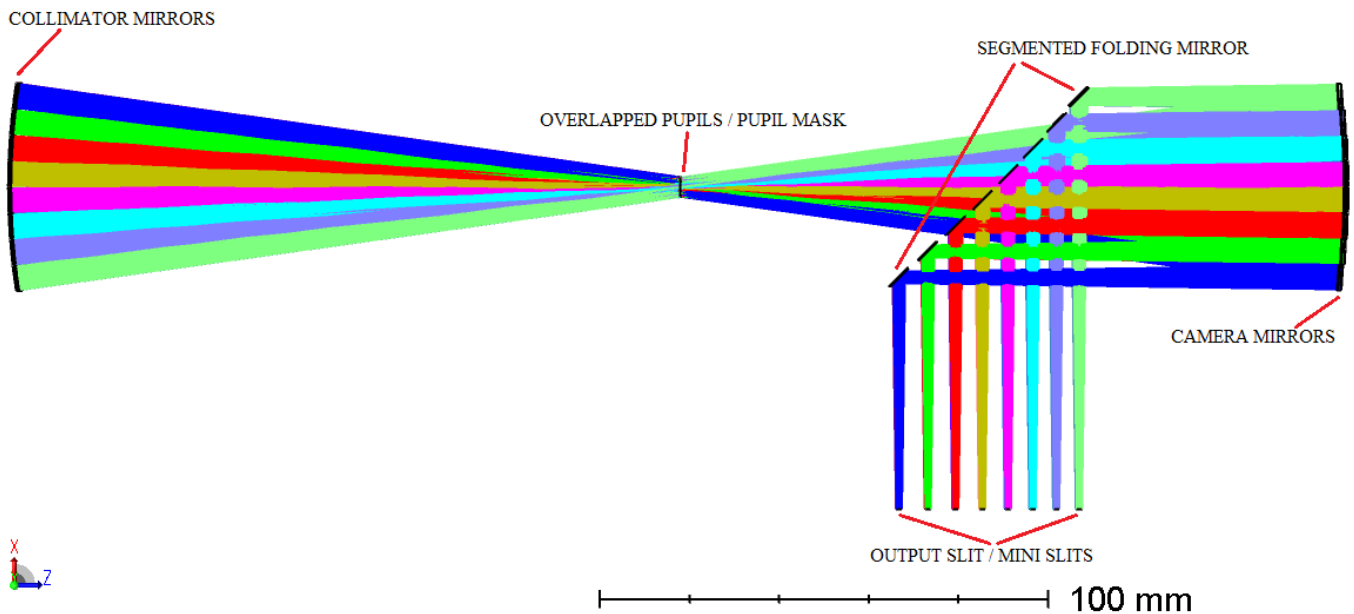


Figure 8 Top view

Table 5. Slicer array parameters

dec. X	dec. X	dec. X	dec. X	dec. X	dec. X	dec. X	dec. X	dec. X	dec. X	dec. X	dec. X	dec. X	dec. X	dec. X	dec. X
0.0000	0.0000	0.0000	0.0000	0.0000	0.0000	0.0000	0.0000	0.0000	0.0000	0.0000	0.0000	0.0000	0.0000	0.0000	0.0000
dec.Y	dec.Y	dec.Y	dec.Y	dec.Y	dec.Y	dec.Y	dec.Y	dec.Y	dec.Y	dec.Y	dec.Y	dec.Y	dec.Y	dec.Y	dec.Y
0.0175	0.0525	0.0875	0.1225	0.1575	0.1925	0.2275	0.2625	-0.0175	-0.0525	-0.0875	-0.1225	-0.1575	-0.1925	-0.2275	-0.2625
tilt X	tilt X	tilt X	tilt X	tilt X	tilt X	tilt X	tilt X	tilt X	tilt X	tilt X	tilt X	tilt X	tilt X	tilt X	tilt X
1.9123	1.9034	1.8953	1.8878	1.8811	1.8751	1.8698	1.8652	-1.9123	-1.9034	-1.8953	-1.8879	-1.8811	-1.8751	-1.8698	-1.8652
tilt Y	tilt Y	tilt Y	tilt Y	tilt Y	tilt Y	tilt Y	tilt Y	tilt Y	tilt Y	tilt Y	tilt Y	tilt Y	tilt Y	tilt Y	tilt Y
-3.8933	-2.7767	-1.6643	-0.5545	0.5545	1.6643	2.7766	3.8931	-3.8933	-2.7767	-1.6643	-0.5545	0.5545	1.6643	2.7766	3.8931

Due to the smaller thickness of the slices, the diffraction effects are more important. The collimator mirrors are, in consequence, asymmetrical with a size of 5.7 mm width x 13.4 mm high. The arrays are separated by 20 mm because RS2 is placed between the arrays. Figure 9 shows the comparison between the Zemax footprint and the diffractive beam simulation at one of the collimator mirrors. For the pupil masks, the pupil diameter is 13.37 mm for to the main lobe diffractive beam diameter at the wavelength of 1565 nm, and 9.26 mm at 1083 nm.

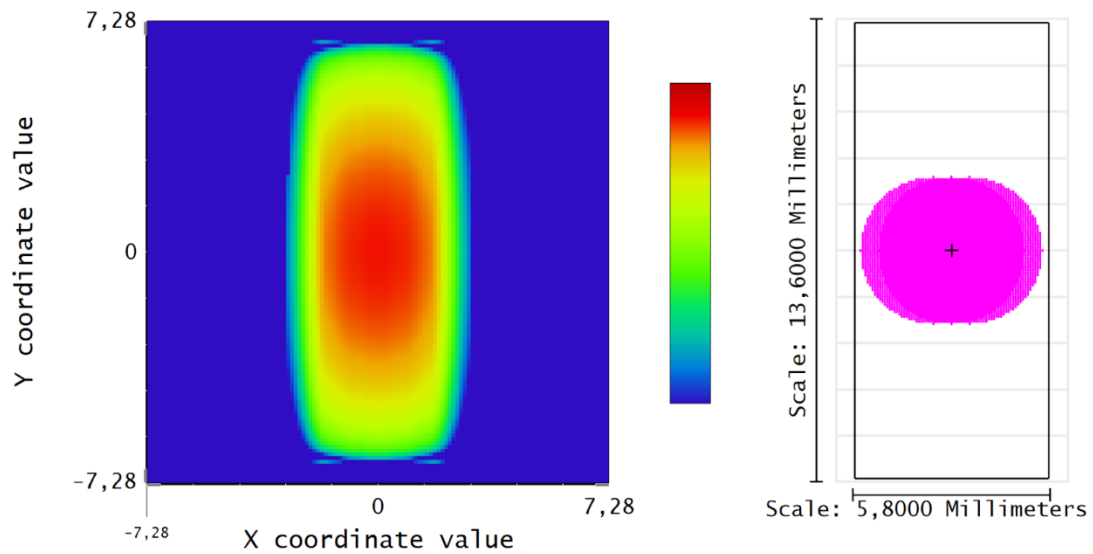


Figure 9 Diffraction simulation vs footprint at collimator

The output mini-slits are formed after a folding mirror. This mirror is segmented into an array of mirrors to be able to compensate the focus differences among the mini-slits. All the segments keep the same tilt of 45 degrees, but they are displaced along Z-axis in order to set the best focus at the output slit, for every mini-slit. The tilt of the mini-slits is measured, as they shall be perpendicular to the ruling of the spectrograph grating, as discussed before. The maximum tilt, respect to the horizontal axis, is lower than 0.004 mm, as shown in Figure 10.

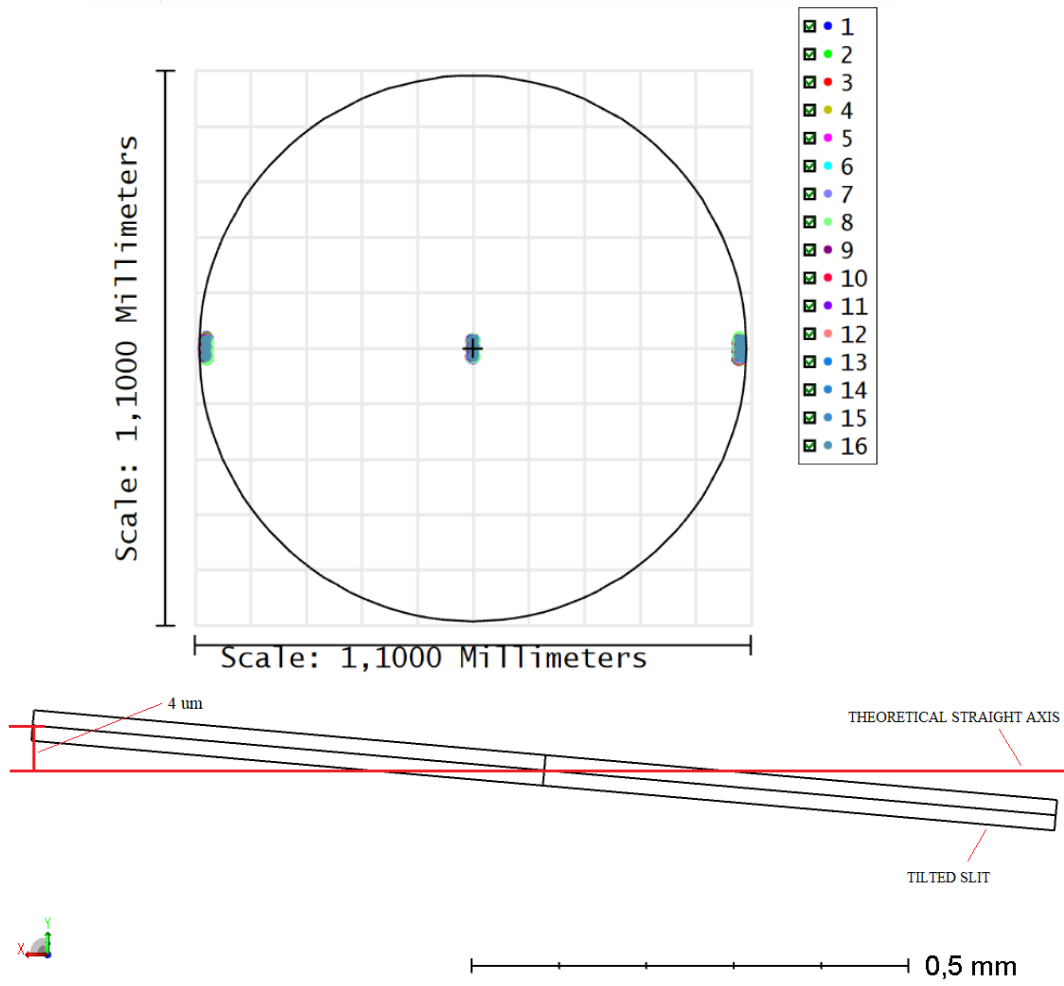


Figure 10 Maximum tilt of the mini-slits

2.3 Expected performance

The designs are diffraction limited, as shown in the Figures 11 and 12, for the metallic and glass slicer, respectively. They show the spot diagrams at the image plane for every mini-slit and for 9 field points distributed over the FOV. It can be seen that the aberrations grow faster in the Figure 12, due to a smaller focal length of the mirrors.

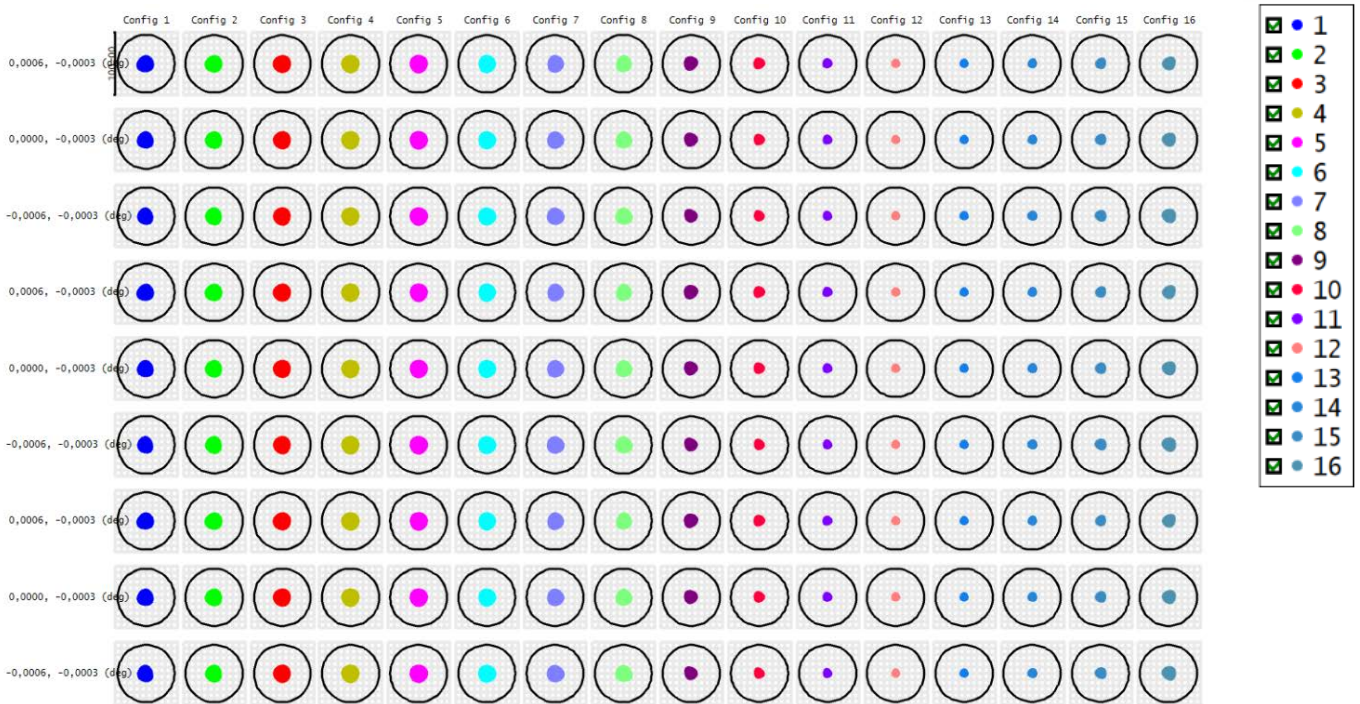


Figure 11 Spot diagram for the metallic slicer

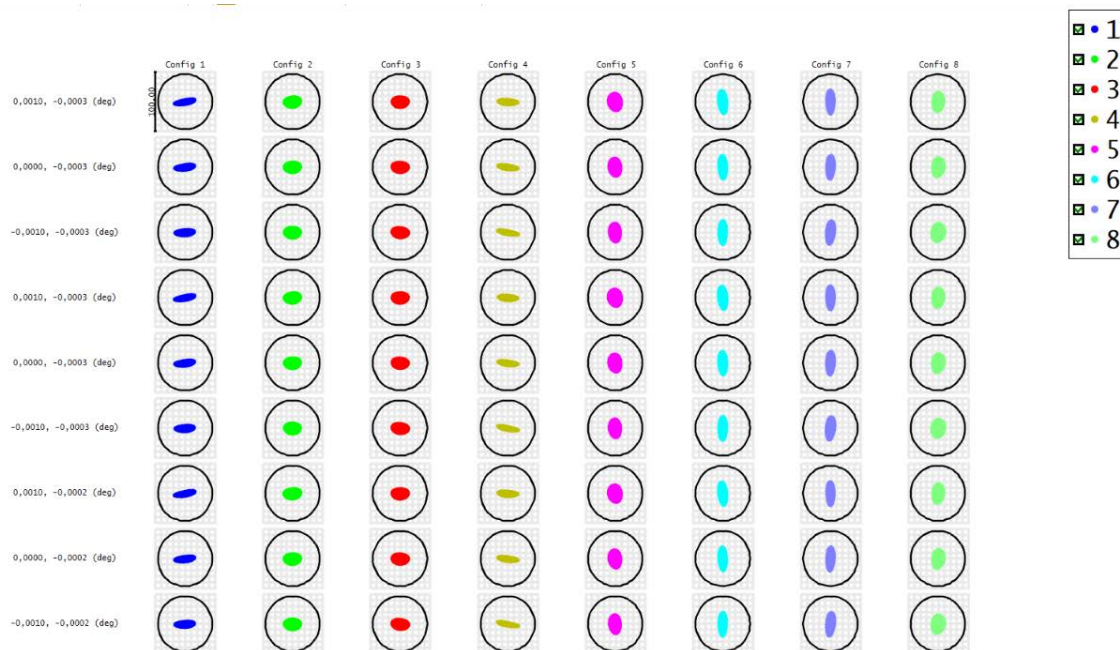


Figure 12 Spot diagram for the glass slicer

Figures 13 and 14 show the pupil images overlapped at the spectrograph's diffraction grating for the metallic and glass slicer, respectively. They represent the footprint ring of every pupil image on a simulated diffraction grating surface. The maximum deviation among the pupils from every mini-slit is 0.539 mm and 0.575 mm for the metallic and glass slicer, respectively.

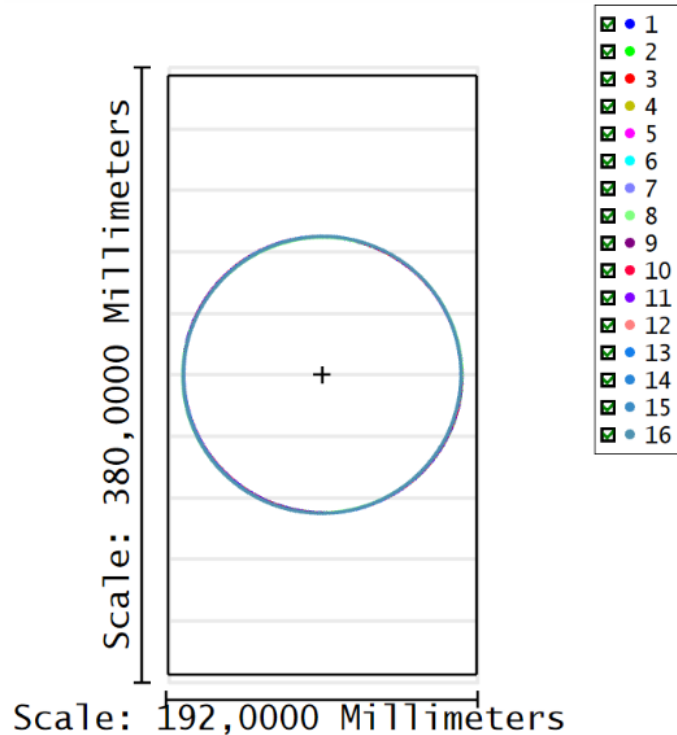


Figure 13 Pupil footprint rings at the diffraction grating for the metallic slicer

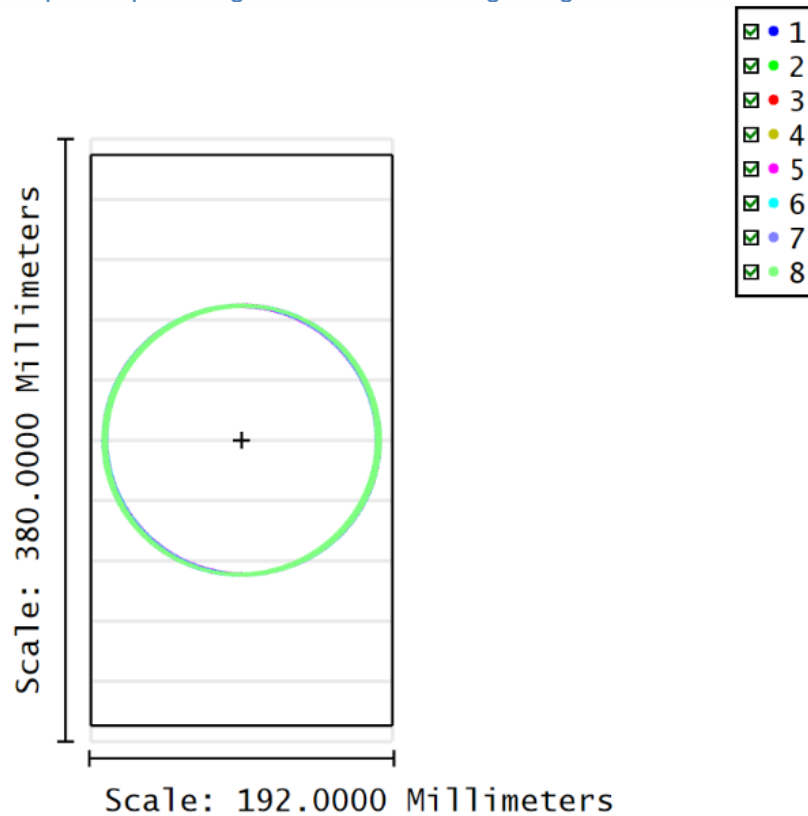


Figure 14 Pupil footprint rings at the diffraction grating for the glass slicer.

3. Conclusions

The optical design for the two alternatives of image slicers, the metallic and the glass one, has faced the challenge of small FOVs, as a result of increasing the spatial resolution. The main drivers of the design have been the optimization in terms of increasing the FOV to a maximum while keeping the compatibility with GRIS. Both, in compromise with telecentricity, diffraction effects and aberrations. Due to the difference in the thicknesses, and thus FOV, the resultant designs are different. The design for the glass image slicer produce an output slit formed with two rows of 8 alternated mini-slits, while the metallic one produces two slits for a total of 16 mini-slits. The performance of the designs has been evaluated in terms of the aberrations, and looking at the light footprint over the simulated GRIS grating, which is at the pupil plane. The next step is to run the tolerance analysis and the evaluation from the partners that will manufacture them.

References

RD1	SOLARNET-FP7 Deliverable 60.9 "Image slicer prototype"
RD2	SOLARNET-FP7 Deliverable 60.10 "Image slicer prototype: tests report"
RD3	GREST Deliverable 4.2 "Multi-slit IFU impact on other optical elements"
RD4	GREST Deliverable 4.3 "Multi-slit IFU preliminary optical design"
RD5	Collados, M., López, R., Páez, Hernández, E., Reyes, M., Calcines, A., Ballesteros, E., Díaz, J. J., Denker, C., Lagg, A., Schlichenmaier, R., Schmidt, W., Solanki, S. K., Straameier, K. G., von der Lühe, O., Volkmer, R., "GRIS: The GREGOR Infrared Spectrograph", <i>Astronomische Nachrichten</i> , Vol. 333, Issue 9, p.872 (2012).
RD6	SOLARNET-H2020 Deliverable 6.2 Validation of the ability to manufacture thin glass slices
RD7	Zero Invar IC-ZX (SHINHOKOKU Steel CO.)